Supporting Information

DNA Translocations through Solid-State Plasmonic Nanopores

Francesca Nicoli, Daniel Verschueren, Misha Klein, Cees Dekker and Magnus P. Jonsson[‡]*

Department of Bionanoscience, Kavli Institute of Nanoscience, Delft University of Technology, Lorentzweg 1, 2628 CJ Delft, The Netherlands

*Corresponding author: MP Jonsson, magnus.jonsson@liu.se

[‡] Present address: Organic Electronics, Department of Science and Technology, Campus Norrköping, Linköping University, SE-60174 Norrköping, Sweden

This supporting information contains:

A – Temperature-dependence of buffer conductivity
B – Current-voltage characteristics
C - Results from additional experiments
D - Temperature-regulated nanopore measurements
E - Estimation of capture distances
F - Discussion on temperature effects on translocation times

A - Temperature-dependence of buffer conductivity

The buffer conductivity at different temperatures was measured using a zeta potential analyzer (Zetasizer Nano, Malvern Instruments Ltd, UK) and fitted to linear curves, as shown below.*

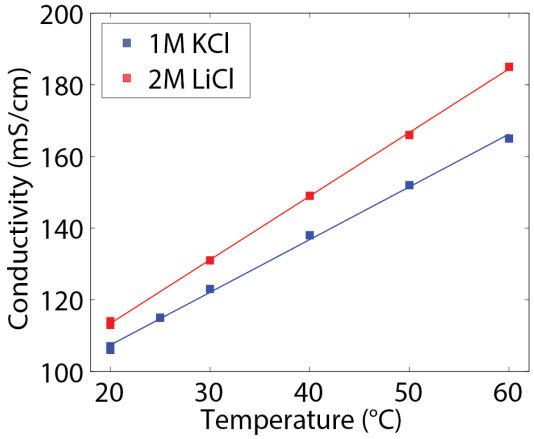

Figure S1. Measured bulk conductivity, σ_{bulk}, of 1M KCl (blue squares) and 2M LiCl (red squares) as a function of temperature. In this temperature range, the experimental values fit well to a linear model, $\sigma_{bulk}(T)=a+bT$, for both buffers. The fits give a=77.9mS/cm, b=1.47mS/(cm×°C) for 1M KCl and a=77.9mS/cm, b=1.78mS/(cm×°C) for 2M LiCl.

B - Current-voltage characteristics

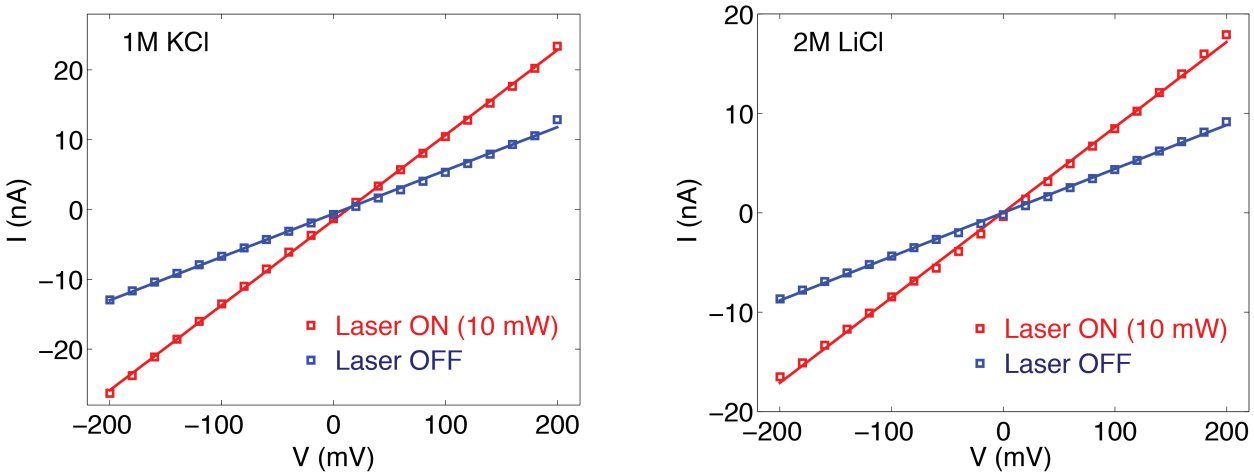

Figure S2. Current versus voltage with (red) and without (blue) laser excitation, in 1M KCl (left) and 2M LiCl (right).

*At the time of proof reading of this paper, a new measurement of the bulk conductivity of 1 M KCl using a micropore indicated a slightly stronger temperature dependence of the buffer bulk conductivity compared with the results obtained with the Zetasizer Nano. We note that such potentially stronger temperature dependence would slightly lower the estimated plasmonic heating temperatures, but not affect the main conclusions of the paper.

C - Results from additional experiments

Event rate upon plasmon excitation in 1 M KCl

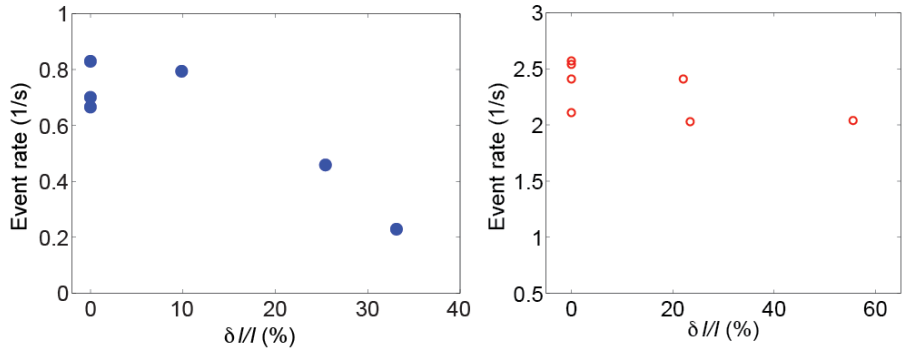

Figure S3. Examples of event rate measurement for a plasmonic nanopore in 1 M KCl versus δI/I. The plots on the left and on the right correspond to measurements where plasmons were excited with longitudinal and transverse polarization, respectively. For both measurements, DNA molecules were translocated from the side of the bowtie antenna at a concentration of 10 ng/μL.

Plasmon-induced rate enhancement in 2M LiCl for different initial rates

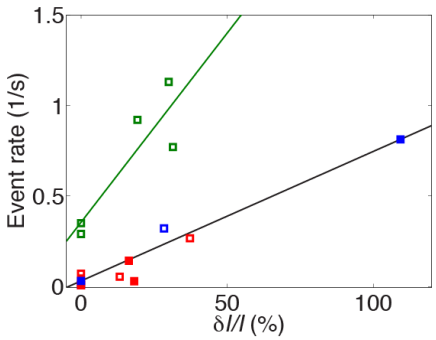

Figure S4. Event rate in 2 M LiCl for experiments with significantly different initial rates at 0 mW, as a function of the relative current increase upon laser illumination. Different colors correspond to different samples. Filled and open symbols correspond to laser illumination in longitudinal and transverse polarization respectively. The full lines are guides to the eye.

Plasmon-induced rate enhancement in 1M LiCl

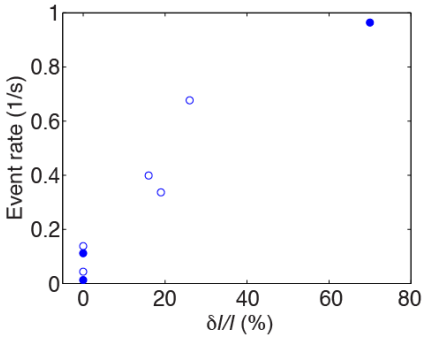

Figure S5. Event rate as a function of the increase in open pore current upon laser illumination in 1 M LiCl buffer. The open and filled symbols correspond to laser illumination in transverse and longitudinal polarization, respectively.

Voltage-dependence on the event rate in 2 M KCl

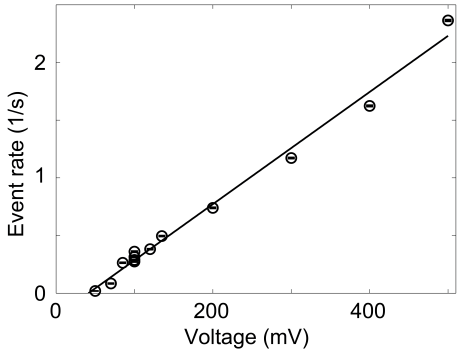

Figure S6. Dependence of bias voltage on the event rate of lambda-DNA translocations in 2 M LiCl.

TEM images before and after measurement for a relatively unstable device

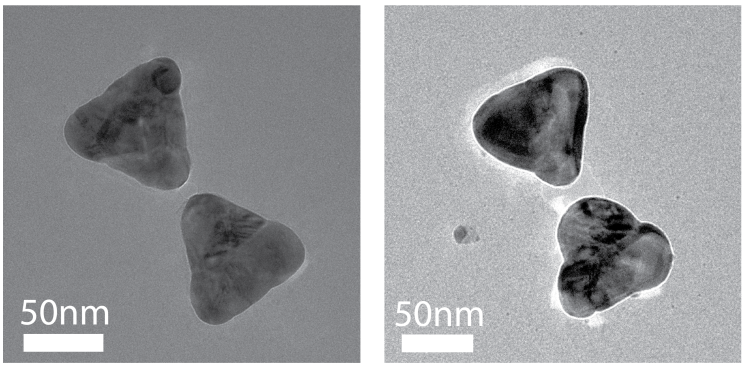

Figure S7. TEM images of a plasmonic nanopore before (left) and after (right) measurement in 1 M KCl. The sample was illuminated in longitudinal mode at 5 mW for a short time (30 s), and in transverse mode for a prolonged period (5 min). This particular chip showed unusually strong nanopore growth during experiment. Small changes in the rounding of the gold triangles can also be observed. Most samples are much more stable.

Event rate-enhancement in 2M LiCl for a locally heated conventional nanopore

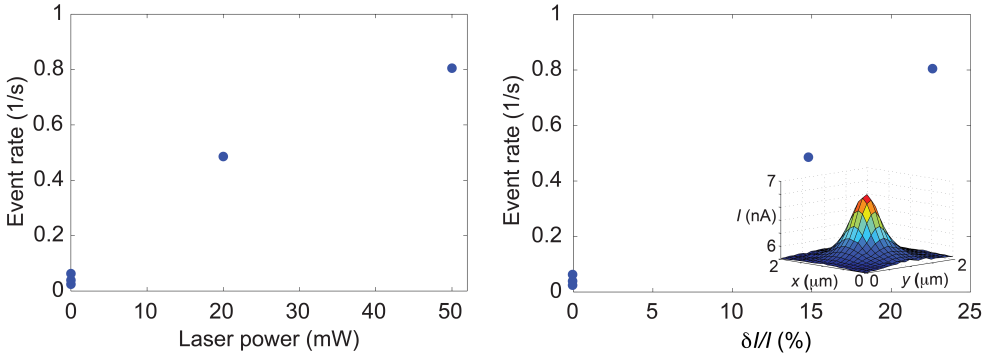

Figure S8. Event rate as a function of laser power (left) and relative increase in the open pore current (right) upon focused laser illumination for a conventional nanopore in 2 M LiCl. The inset shows a 2D current scan through the focal plane obtained at 20 mW and at 100 mV bias voltage.

D - Temperature-regulated nanopore experiments

Temperature effects on DNA translocations through a conventional nanopore were investigated in a measurement setup that provides control of the temperature of the whole flow cell using a Peltier heater/cooler. The nanopore current was monitored in the same way as for the plasmonic measurements. The nanopores also had the same dimensions (10 nm in diameter, 20 nm thick SiN membrane) as in the plasmonic measurements, but without the gold nanoantennas and a slightly different geometry of the chip in the region outside the membrane (where instead of a SiO_2 layer between the membrane and the Si, we used two SiO_2 and SiN layers above the nanopore membrane). All measurements were acquired using a 100 mV bias voltage.

Temperature-dependence of absolute and relative conductance blockades

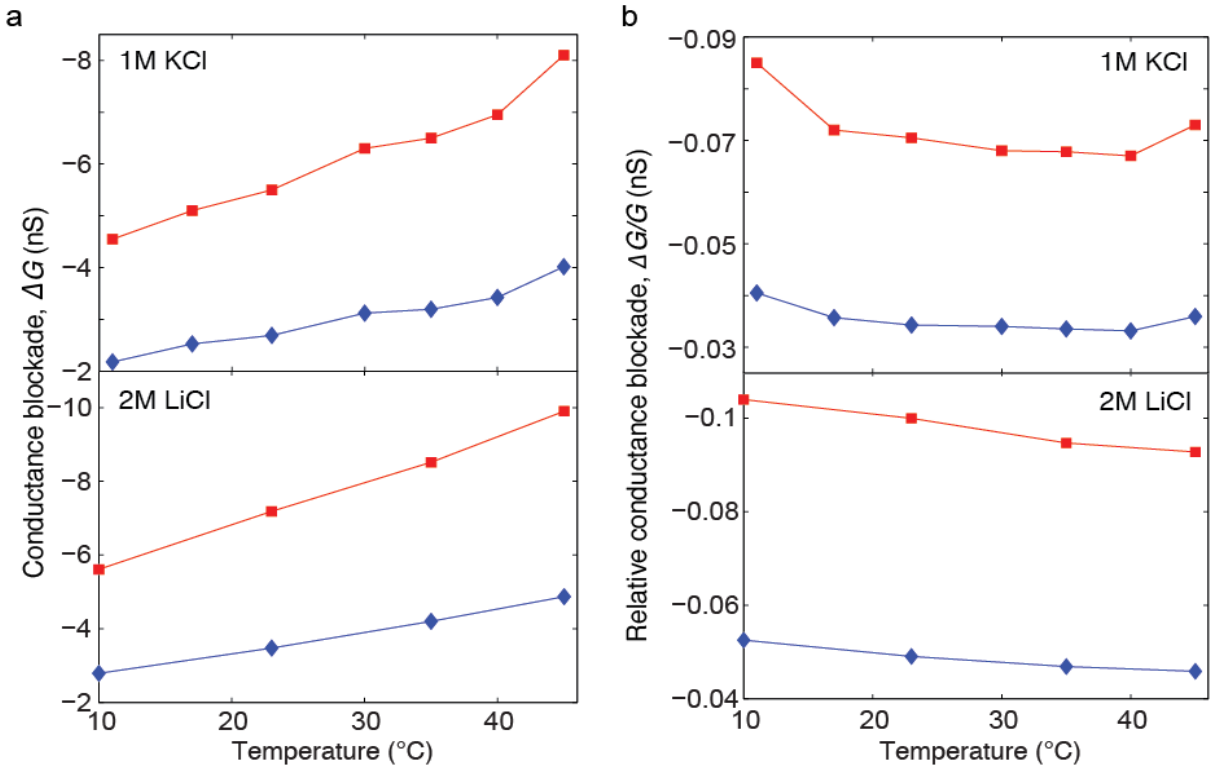

Figure S9. **a)** Conductance blockade versus temperature for lambda-DNA in 1 M KCl (top) and 2 M LiCl (bottom). Blue diamonds and red squares correspond to the first and the second peak of the conductance histograms, respectively, similar to the plasmonic measurements. **b)** Same as in a), but for the relative conductance blockade.

Comparison of temperature-induced and plasmon-induced enhancement of the event rate

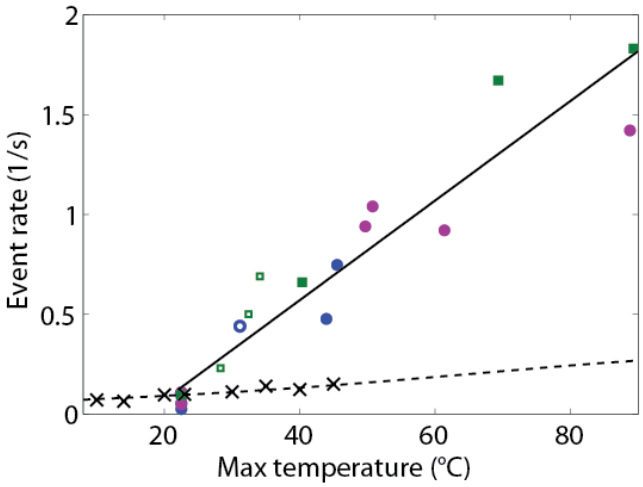

Figure S10. Comparison between event rate for plasmonic excitations (colored symbols and black full line) and uniform heating (black x symbols and dashed line). All experiments were performed in 2 M LiCL. Different colors correspond to different plasmonic nanopores. Filled and open symbols are for longitudinal and transverse polarization, respectively. Squares and circles correspond to DNA added from the side of the bowtie antenna and the other side, respectively. The x-axis shows the measured temperature for the temperature-regulated measurements and the estimated maximum temperature for the plasmonic measurements, assuming that $\delta I/I$ can be fully ascribed to plasmonic heating and using the temperature dependence of the buffer conductivity, as shown in Fig. S1.

Temperature dependence of event rate in 1M KCl for a uniformly heated pore.

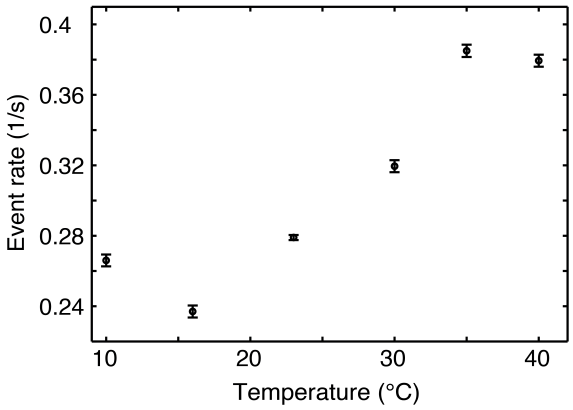

Figure S11. Temperature dependence of the event rate in 1M KCl upon uniform heating of a conventional nanopore.

E - Estimation of electrophoretic capture distances

Here we estimate the electrophoretic capture distance, i.e. the typical distance from the pore at which DNA molecules are electrophoretically captured and pulled through the nanopore. The different parameters are approximated at 25 °C for 1 M KCl and 2 M LiCl and are stated in parentheses when introduced. According to Grosberg and Rabin,[1] the electrophoretic capture distance, r_C, can be estimated as

$$r_C = \Delta V \frac{d^2 \mu}{8 l D}$$

where ΔV is the applied voltage over the membrane (0.1 V), d is the diameter of the nanopore (10 nm), l is the effective length of the pore (8.6 nm, adopted from Kowalczyk et al.[2] for the same membrane thickness), μ is the electrophoretic mobility of the DNA molecule in the particular electrolyte and D is the DNA diffusion coefficient. The diffusion coefficient can be estimated using[3]

$$D = \frac{8\sqrt{3\pi} k_B T}{18\pi\eta\sqrt{l_p l_C}}$$

where k_B is the Boltzmann constant (1.38×10^{-23} $kgm^2s^{-2}K^{-1}$), T is the absolute temperature (298.15 K), η is the viscosity of the electrolyte (0.88 mPa×s for 1 M KCl[4] and 1.2 mPa×s for 2 M LiCl),[5] l_p is the DNA persistence length (48.5 nm)[6] and l_C is the DNA contour length (16 µm). This gives estimated diffusion coefficients of 2.3 $\mu m^2/s$ and 1.7 $\mu m^2/s$ in 1 M KCl and 2 M LiCl, respectively. The electrophoretic mobility can be estimated using

$$\mu = \frac{2\alpha e r_D}{\pi\eta f d}$$

where e is the elementary charge (1.6×10^{-19} $kgm^2/(Vs^2)$), r_D is the Debye length, (0.3 nm for 1 M KCl and 0.2 nm for 2 M LiCl),[7] f=0.34 nm is the distance between base pairs and d is the diameter of the DNA molecule (2 nm). The numerical factor α accounts for the fact that the effective charge of the DNA is lowered due screening by counterions. We use α=0.5 for 1 M KCl, and estimate α=0.07 in 2 M LiCl, which is 7 times than in 1 M KCl, based on a stronger binding of Li+ ions than K+ ions to the DNA, resulting in a much higher screening.[8] Using these values, the electrophoretic mobilities can be estimated to 1.7×10^{-8} $m^2/(V\times s)$ and 0.17×10^{-8} m^2/Vs for 1 M KCl and 2 M LiCl, respectively.

Finally, we estimate the capture distances to be 1.0 µm and 150 nm for 1 M KCl and 2 M LiCl, respectively. While being rough estimations, based on treating the DNA molecule as a point particle (which particularly may not hold for small capture distances), we conclude that the capture distance is almost one order of magnitude smaller for 2 M LiCl compared with 1 M KCl. As a result, local heating effects will play a significantly larger role in measurements in 2 M LiCl, in agreement with the effects we observe on the event rate.

F - **Discussion on temperature effects on translocation times**

In this section we consider how the DNA translocation times depend on a localized temperature change near the pore. The DNA translocation times are determined by a force balance between a forward electrophoretic drive and a retracting viscous drag on the DNA. The viscous drag force consists of two parts: a viscous drag force on the DNA strand residing in the pore and a viscous drag on the untranslocated part of the DNA away from the pore (on the order of the radius of gyration, roughly 500 nm).[9] Drag forces in general can be described as

$$f_d = \xi \eta v_d \tag{1}$$

where v_d is the relevant velocity, η is the buffer viscosity (locally in the pore or at the region of the untranslocated DNA), and ξ is a geometrical factor characterizing the size of the object that the drag force is exerted on (hence, different for the two drag contributions). The viscosity decreases with increasing temperature for our buffer conditions.[4, 5] While this may indicate that the drag forces decrease with temperature, we also need to consider how the relevant velocities depend on temperature.

Importantly, the relevant velocity is different for the untranslocated DNA and for the DNA inside the pore. In a simplified model, the velocity scale that determines the drag on the untranslocated part of the DNA is set by the DNA translocation speed, whereas the velocity scale that determines the drag in the pore is set by the electroosmotic flow (EOF) in the pore.[10] The EOF arises from a net charge flow in the mobile Debye layer near the pore walls and is, at the center of the pore, given by[11, 12]

$$v_{EOF} = \frac{\Delta V \epsilon_0 \epsilon_r \Phi_0}{l\eta} \tag{2}$$

Here, ΔV *is* the applied voltage bias, $\epsilon_r \epsilon_0$ is the electric permittivity of water, l is the pore length and Φ_0 is the zeta-potential at the pore wall. The Grahame equation connects the surface charge density and the potential on the pore wall[13]

$$\sigma_{\text{surf}}(\Phi_0) = \frac{2\epsilon_0 \epsilon_r k_B T}{e r_D} \sinh\left(\frac{e\Phi_0}{2k_B T}\right) \tag{3}$$

Here, σ_{surf} is the surface charge density on the pore wall, k_B is the Boltzmann constant, T is the temperature, e the electron charge, and r_D is the Debye length (which has a negligible dependence on temperature in this case). Upon linearizing equation (3) for small zeta-potential, the EOF will be given by

$$v_{EOF} = \frac{\Delta V \sigma_{\text{surf}} r_D}{l\eta} \tag{4}$$

where an appreciable temperature dependence of the EOF is enclosed in the viscosity only.

The EOF will exert a drag force on the DNA if the pore surface is negatively charged (as is the case for SiN at pH 8). We note that the EOF is typically much faster than the DNA translocation speed (on the order of 10^{-1} m/s compared to 10^{-3} m/s for the DNA translocation speed for a typical surface charge density of -60 mC/m^2)[10]. As a result, the EOF dominates and determines the drag force on the DNA inside the pore. In turn, the inverse proportionality of this flow to the buffer viscosity cancels the initial dependence of the drag force on viscosity (equation 1). Hence, the drag force in the pore due to the EOF will be unaffected by a change in viscosity and in turn, this force will be largely unaffected by a change in temperature.

Based on this reasoning, we conclude that local heating of the nanopore is not expected to significantly affect the translocation time. By contrast, uniform heating affects the viscosity also in the region of the untranslocated DNA, and the resulting decrease in the drag force on the untranslocated DNA will thus be compensated by an increase in the relevant velocity scale, which in this case is the DNA translocation speed. Hence, uniform heating, but not local heating, is expected to result in decreased translocation times, which is in agreement with our observations.

References

1. Grosberg, A. Y.; Rabin, Y. *J. Chem. Phys.* 2010, 133, (16), 165102.
2. Kowalczyk, S. W.; Grosberg, A. Y.; Rabin, Y.; Dekker, C. *Nanotechnology* 2011, 22, (31), 315101.
3. Plesa, C.; Kowalczyk, S. W.; Zinsmeester, R.; Grosberg, A. Y.; Rabin, Y.; Dekker, C. *Nano Lett.* 2013, 13, (7), 3445-3445.
4. Afzal, M.; Saleem, M.; Mahmood, M. T. *Journal of Chemical and Engineering Data* 1989, 34, (3), 339-346.
5. Abdulagatov, I. M.; Zeinalova, A. B.; Azizov, N. D. *Journal of Molecular Liquids* 2006, 126, (1-3), 75-88.
6. Geggier, S.; Kotlyar, A.; Vologodskii, A. *Nucleic Acids Res.* 2011, 39, (4), 1419-1426.
7. Israechvili, J. N., *Intermolecular and surface forces*. 3 ed.; Academic Press Inc.: 2011.
8. Kowalczyk, S. W.; Wells, D. B.; Aksimentiev, A.; Dekker, C. *Nano Lett.* 2012, 12, (2), 1038-1044.
9. Chen, L.; Conlisk, A. T. *Biomed. Microdevices* 2011, 13, (2), 403-414.
10. He, Y.; Tsutsui, M.; Fan, C.; Taniguchi, M.; Kawai, T. *Acs Nano* 2011, 5, (10), 8391-8397.
11. Ghosal, S. *Phys. Rev. Lett.* 2007, 98, (23), 238104.
12. Wong, C. T. A.; Muthukumar, M. *J. Chem. Phys.* 2007, 126, (16), 164903.